DE GRUYTER OPEN

Acta Geophysica
vol. 64, no. 6, Dec. 2016, pp. 2051-2076
DOI: 10.1515/acgeo-2016-0086

Shear Wave Velocity Estimates through Combined Use of Passive Techniques in a Tectonically Active Area

Rajib BISWAS[1] and Saurabh BARUAH[2]

[1]Department of Physics, Tezpur University, Tezpur, Assam, India;
e-mail: rajib@tezu.ernet.in

[2]Geoscience Division, CSIR-NEIST, Jorhat, Assam, India

A b s t r a c t

We made an attempt to assess the shear wave velocity values V_S and, to a lesser extent, the V_P values from ambient noise recordings in an array configuration. Five array sites were situated in the close proximity to borehole sites. Shear wave velocity profiles were modeled at these five array sites with the aid of two computational techniques, viz. spatial autocorrelation (SPAC) and H/V ellipticity. Out of these five array sites, velocity estimates could be reliably inferred at three locations. The shear wave velocities estimated by these methods are found to be quite consistent with each other. The computed V_S values up to 30 m depth are in the range from 275 to 375 m/s in most of the sites, which implies prevalence of a low velocity zone at some pocket areas. The results were corroborated by evidence of site geology as well as geotechnical information.

Key words: array recordings, SPAC, ellipticity.

1. INTRODUCTION

Seismic hazard estimation in recent years has received vast attention from all levels, starting from geo-scientists, civil engineers and policy makers (Hartzell *et al.* 1996, Yamanaka *et al.* 1993, 1994, 1998; Köhler *et al.* 2007,

Papadopoulou-Vrynioti *et al.* 2013, Pavlou *et al*. 2013, Kassaras *et al.* 2015). The interest in this area is motivated by the notion of minimizing damage by accurate hazard estimation, rather than averting it. One of the important steps in hazard estimates is to reliably determine shear wave velocity profiles. This parameter is basically frequency dependent which is dispersive in nature (Seligson 1970). The dispersive character of shear wave velocity can be efficiently exploited to reveal an underlying one dimensional velocity model, pertaining to a specific study area (Borcherdt 1970, Campbell 1976, Ohnberger *et al.* 2004a, b; Herak 2008). Estimation of a shear wave velocity profile at a site of interest is essential towards the assessment of seismic hazard. The estimations have been performed by making use of data accrued through array implementations.

In our recent work, we estimated the site effect of Shillong area through modified method of Nakamura (Biswas and Baruah 2011). More specifically, Biswas *et al.* (2013) investigated attenuation and site effect in Shillong area using microtremors. More recently, mapping of sediment thickness has also been accomplished (Biswas *et al.* 2015). Microtremor data obtained by an array of sensors have been proven an effective tool for estimation of shear wave velocity (Williams *et al.* 2003). The most widely used techniques for the evaluation of shear wave velocity from dispersive velocity curves of microtremor propagation are the spatial auto-correlation technique (Okada 2006), the frequency wavenumber method (Seligson 1970, Bozdag and Kocaoglu 2005) and the H/V spectral ratio can be modeled by the theoretical ellipticity of layered velocity models (Claprood and Asten 2007a, b). All these three passive techniques possess different methodology for attaining depth profiles. Despite this, certain researchers combined two of the three to determine the V_S profiles (Fäh *et al.* 2003, Picozzi *et al.* 2005, Di Giulio *et al.* 2006, Claprood and Asten 2007a, b; 2010) and fewer articles regarding adoption of all three passive techniques to attain the shear wave velocity structure (Kuo *et al.* 2009, Boore and Asten 2008).

In this article, we also endeavor to exploit these computing schemes to produce a reliable estimate of velocity to depth profile. Here, we first derive velocity curves through spatial autocorrelation technique. Further, to get more refined and validated results, we compare our finding with all sorts of available geophysical data. The one-dimensional velocity models estimated through these techniques are analyzed in terms of frequency band. Finally, the attained velocity structures are compared for consistency with the models obtained from inversion of ellipticities of Rayleigh wave modes computed from single station three-component horizontal-to-vertical ratio method with simultaneous comparison with the available geotechnical information.

2. GEOLOGICAL BACKGROUND

The study area is located within the Shillong Plateau (SP). The Shillong City, with an area coverage of 6430 km^2 and an average elevation of 1000 m has an approximate population of 180 000. The SP with an Archaean gneissic basement and late Cretaceous–Tertiary sediments along its southern margin is bounded by the Brahmaputra river-fault to the north and the Dauki fault to the south (Kayal *et al.* 2006, Kayal 2008, Rao and Rao 2008). The

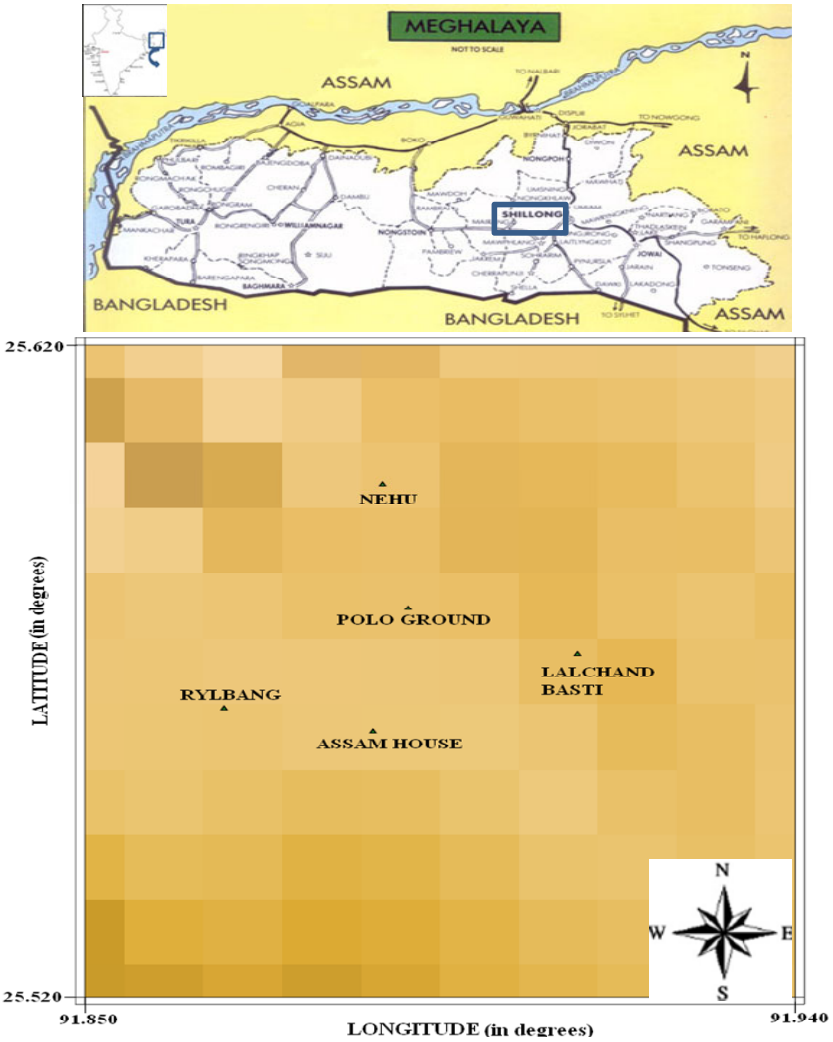

Fig. 1. Locations of the five array sites in Shillong city which is represented by the filled triangles. In inset, map of India is given along with the study area in Meghalaya state.

study area is marked by the Shillong series of parametamorphites, which include mostly quartzites and sandstones, followed by schist, phyllites, slates, *etc.* (GSI 1985). A conglomerate bed containing cobbles and boulders of Archaean crystalline mainly constitutes Shillong series of rocks. The Shillong series grew as depositions in shallow marine conditions over these Archean crystalline rocks (Sar 1973, Mitra and Mitra 2001). The Shillong groups of rocks are intruded by epidiorite rocks, known as Khasi Greenstone as outlined in Fig. 1. The Khasi Greenstone is a group of basic intrusives in the linear to curvilinear form occurring as concordant and discordant bodies within the Shillong group of rocks and suffered metamorphism (Srinivasan *et al.* 1996). These rocks are widely weathered and the degree of weathering is mainly found in the topographic depressions. The metabasic rocks are more prone to weathering than the quartzite rocks. Additionally, the low lying areas are filled with valley fill sediments. Numerous lineaments trend in NE-SW, N-S, and E-W directions in the area (Chattopadhaya and Hashimi 1984).

3. ARRAY CONFIGURATION AND DATA

Array records of ambient noise are used to obtain the shear wave velocity structure of both shallow and deep sedimentary layers. In order to record ambient noise, an array consisting of four sensors was laid out at five selected locations which were located in close proximity to the borehole logs in Shillong City. These five locations were chosen as they cover most characteristic subsurface profiles pertinent to Shillong City (see Table 1 for station locations). For each of them, a homogeneous instrumentation was implemented with good soil sensor coupling (see Bard 2004). It comprised of three Kinematrics Trillium 120P sensors and one short period S-13 Teledyne Geotech, all operating at a sampling rate of 100 samples/s. The time synchronization was provided for each station by GPS receivers. We implemented an equilateral triangular array with three sensors laid out at the

Table 1

Station locations

Station name	Latitude [°]	Longitude [°]	Elevation [m]
Assam House	25.567	91.892	1544
Lalchand Basti	25.590	91.915	1456
Rylbang	25.574	91.880	1562
Nehu	25.611	91.901	1427
Pologround	25.580	91.888	1444

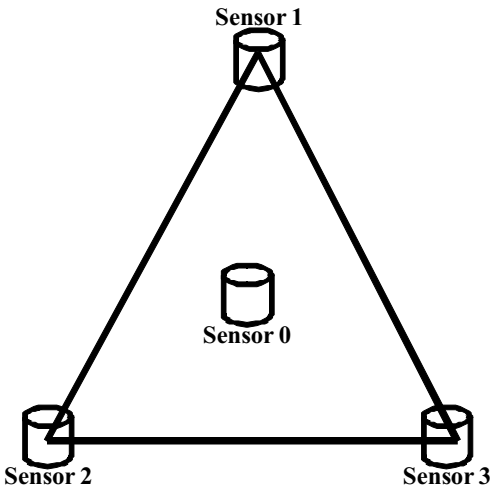

Fig. 2a. Deployed array layouts at the five noise recording site. Here, four sensors are provided. The formation is an equilateral triangle. At the incentre, there remains the central sensor, surrounded by the remaining three sensors. The aperture is 8.67 m whereas the array radius is kept at 5 m.

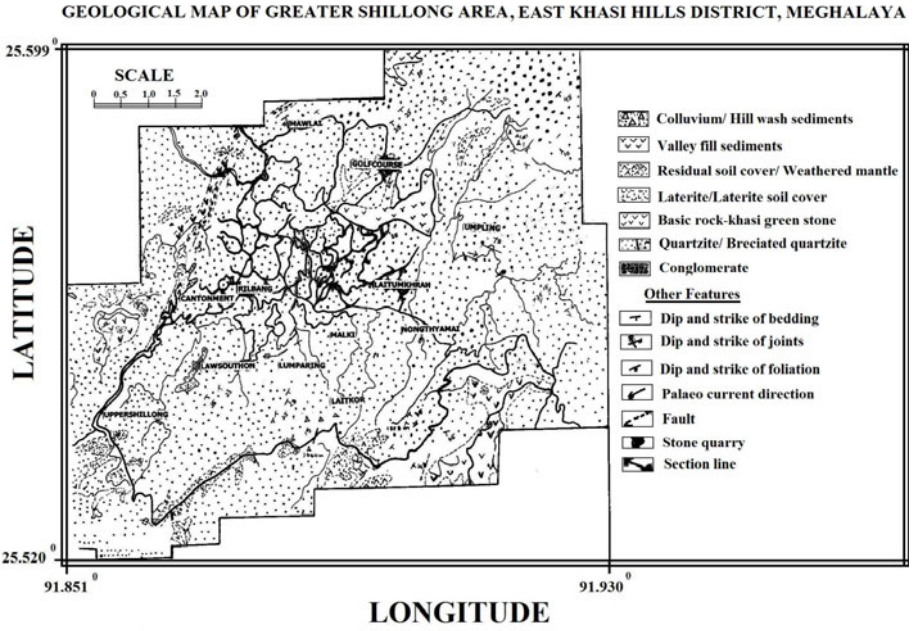

Fig. 2b. Geological map of Shillong City (after GSI 1985). The scale shown in the figure is in kilometres.

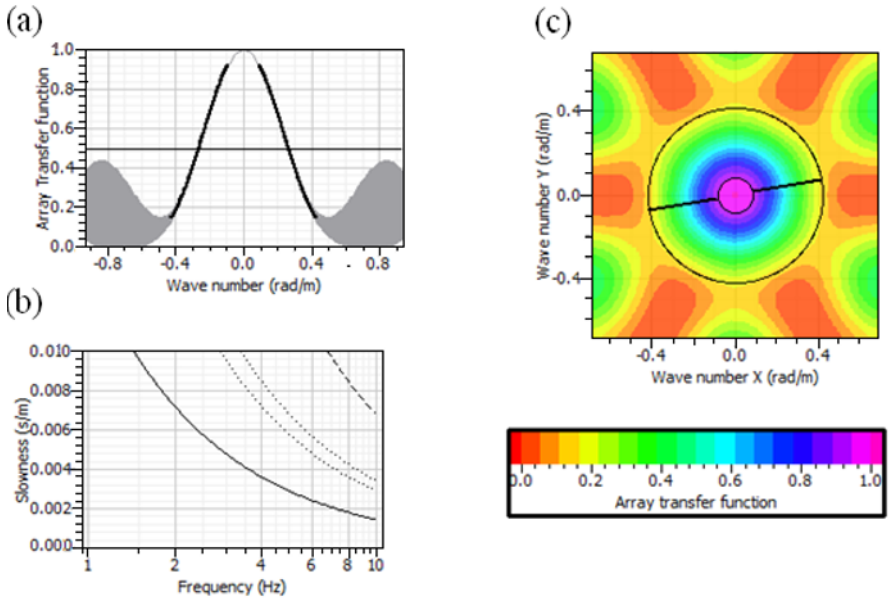

Fig. 3. Theoretical array response for the adopted array layout: (a) Plot of array transfer function *versus* wavenumber. The single peak appearing here corresponds to the main peak. The other side lobes represent the aliasing peaks; (b) Array responses computed for the whole frequency band. k_x and k_y values are plotted along the horizontal and vertical axis, respectively. The color scale indicates the values of array transfer function; (c) Slowness *versus* frequency curve within the defined limits. The four exponential lines represent the constant wavenumber values. $k_{min}/2$ (continuous line), k_{min} (dot-dash line), $k_{max}/2$ (dots), and k_{max} (dashed line).

vertices, while the fourth was placed at the centre of the triangle. Initially, two different arrays were designed with radius of 1 and 5 m. However, surface wave dispersion characteristics obtained by the array of radius of 1 m could not be utilized due to poor resolution in all five sites, while better resolution of dispersion characteristics was achieved for the array of radius of 5 m. Thus, the ambient noise wavefields from 5 m radius array was the prime input towards the estimation of the velocity profile. Consequently, the aperture is kept equal to 8.67 m. Figure 2a shows the adopted layout in selected locations in Shillong City.

The arrays with similar configuration were deployed at five locations, *i.e.*, ASSAM HOUSE, POLOGROUND, NEHU, LALCHAND BASTI, and RYLBANG, as demonstrated in Fig. 2b. The array transfer function, as proposed by Woods and Lintz (1973) is defined within the wave number limits k_{min} and k_{max} and is described in the k_x and k_y plane. Additionally, the corresponding theoretical array response is represented by Fig. 3.

4. SPATIAL AUTOCORRELATION METHOD

The spatial auto-correlation techniques take advantage of the random distribution of sources in time and space to link auto-correlation ratios to phase velocities. In the case of a single-valued phase velocity per frequency band, Aki (1957) demonstrated that these ratios have the shape of Bessel functions of 0 order, the argument of which depends upon the dispersion curve values and the array aperture to reveal the nature of the background seismic noise and also the characteristics of the propagation medium. Bettig *et al.* (2001) brought slightly modified the original formula to extend the method for irregular arrays and urban investigations.

The spatial autocorrelation function of a single plane wave polarized in x direction, $u(x, t)$ for region $x \in [0, X]$ in time domain $t \in [0, T]$ is defined, after Wathelet *et al.* (2004), as follows:

$$\left\langle \varphi(\xi,t) \right\rangle_x = \frac{1}{X} \int_0^X u(x,t)u(x+\xi,t)dx \ . \tag{1}$$

Considering SPAC to be stationary both in space and time, Eq. 1 can be written, after Aki (1957), as

$$\varphi(\xi) = \frac{1}{\pi} \int_0^\infty \varphi(\omega) \cos\left(\frac{\omega}{c(\omega)} \xi \right) d\omega \ , \tag{2}$$

where $\varphi(\omega)$ is the autocorrelation frequency spectrum, ω is the angular frequency, and $c(\omega)$ is the frequency dependent velocity.

From this basic equation, pertaining to the frequency dependent velocity and after adopting the theoretical procedure after Bettig *et al.* (2001), we computed each spectrum pertaining to the array sites deployed at those selective locations. We utilized a window span of ten minutes to evaluate spatial autocorrelation ratio for the respective five sites. After obtaining the dispersion curves, we intend to derive shear wave velocity models, accompanied by V_P values at these five array sites. In addition, the ellipticity peak of fundamental mode of Rayleigh wave corresponding to the estimate of H/V ratio were inverted in order to check the consistency of the inverted results by SPAC. While doing so, as input parameter for the required modeling, we enlist the values of three sites in Tables 2, 3 and 4, respectively, in synchrony with the available borehole information. For the other two sites where no prior information was available regarding depth, the inversion was confined to depth of 30 m only, as given in Table 5. Thus, we attained velocity models for all the five array sites by inverting the dispersion curves of SPAC with the aid of modified neighbourhood algorithom (Sambridge 1999a, b) by Wathelet *et al.* (2004); the results of which are detailed below.

Table 2

Parameterized model for inversion up to a depth of 65 m

Layer	Thickness [m]	V_P [m/s]	V_S/V_P	Poisson's ratio	Density [t/m^3]
Sediments	65 No. of layers 8	200-1275	0.1 to 0.707	0.2 to 0.5	2
Half space	–	2000-3000	0.1 to 0.707	0.2 to 0.5	2

Table 3

Parameterized model for inversion up to a depth of 51 m

Layer	Thickness [m]	V_P [m/s]	V_S/V_P	Poisson's ratio	Density [t/m^3]
Sediments	1 to 51 No. of sub-layers 5	300-1000	0.1 to 0.707	0.2 to 0.5	2
Half space	–	2000-3000	0.1 to 0.707	0.2 to 0.5	2

Table 4

Parameterized model for inversion up to a depth of 100 m

Layer	Thickness [m]	V_P [m/s]	V_S/V_P	Poisson's ratio	Density [t/m^3]
Sediments	1 to 100 No. of sub-layers 5	450-1475	0.1 to 0.707	0.2 to 0.5	2
Half space	–	2250-4200	0.1 to 0.707	0.2 to 0.5	2

Table 5

Parameterized model for inversion for an arbitrary depth of 30 m

Layer	Thickness [m]	V_P [m/s]	V_S/V_P	Poisson's ratio	Density [t/m^3]
Sediments	30 No. of layers 6	200-1000	0.1 to 0.707	0.2 to 0.5	2
Half space	–	2000-3500	0.1 to 0.707	0.2 to 0.5	2

5. VELOCITY PROFILES FROM SPAC FOR EACH ARRAY ASSAM HOUSE

The compressional wave (V_P) and shear wave (V_S) velocity profiles computed for this site are demonstrated in Fig. 4a. The depth of the profile is restricted to 30 m due to lack of *a priori* information of local geology. The shear wave velocity varies between 200 and 400 m/s up to a depth of 30 m, corresponding to the lowest misfit. Gradual increase is observed in V_S, starting from 1 m depth. Corresponding to 1 m stratum of top layer, the shear wave velocity has been estimated at 220 m/s, whereas the V_P value is 500 m/s. In the intermediate layers, with thicknesses of 2 and 4 m, the V_S values are 260 and 310 m/s, respectively. The bottom layer whose thickness is 14 m yields the highest value of shear wave velocity equal to 430 m/s. The dispersion curve yielded by this inversion is also provided in the same figure. The slowness varies between 0.0020 and 0.0032 s/m in the frequency band 0.5 to 10 Hz.

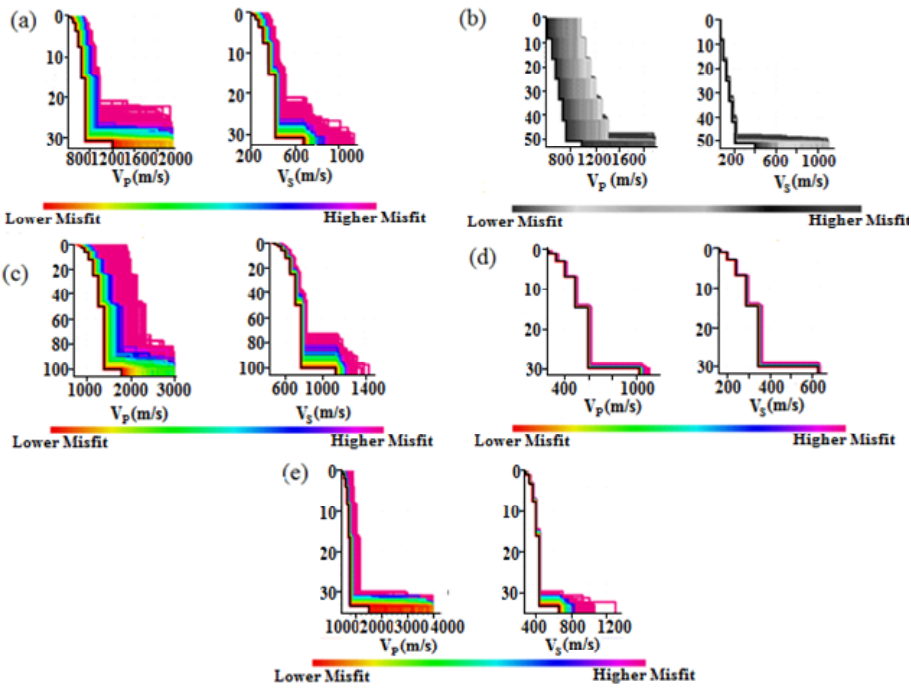

Fig. 4. Shear wave velocity profile estimated from spatial autocorrelation ratios: (a) Assam House, (b) Nehu, (c) Rylbang, (d) Polo ground, and (e) Lalchand Basti.

6. NEHU CAMPUS

This site, as the Assam House, is a plain land formation but with borehole information in its vicinity. Thus, lithological information towards direct inversion of SPAC curves can be incorporated. The velocity profile constrained up to depth of 55 m is illustrated in Fig. 4b. The uppermost layer, having thickness of 8.5 m, produces a very low value of *Vs* which has been estimated at 120 m/s. As for the V_P, it is found equal to 390 m/s. Towards deeper layers, the shear wave velocity is observed to be slowly rising, reaching a value of 210 m/s for the bottom layer. The same trend is observed to the obtained V_P values. These results indicate a low velocity zone at this site. Concerning the computation of the dispersion curve, the slowness is characterized by higher values for the fundamental mode of Rayleigh waves, starting from 0.004 s/m.

7. RYLBANG

This site is located on the outskirts of Shillong City. It is worth noting that there have been borehole drillings in the immediate neighborhood of this site. Owing to this, *a priori* information can be incorporated in parameterization to acquire a reliable velocity structure underneath this site after computation of SPAC curves. On inverting the SPAC curves, the depth profiles obtained are displayed in Fig. 4c. For the uppermost layer, having a thickness of 4 m, V_S is estimated to be in the range of 385 to 525 m/s. Similarly, V_P is observed to be in the range of 600 to 700 m/s for the same layer. Below, along the estimated profile, *Vs* increases in regular intervals, a trend also apparent in the estimates of V_P. For the bottom layer, V_S attains a value of 720 m/s.

The dispersion curve covers the frequency band from 2 to 10 Hz. The slowness estimates for the fundamental mode of Rayleigh wave is found to be lower, compared to the previously mentioned sites.

8. POLO-GROUND

Regarding this site, the shear wave velocity profile has been estimated up to depth of 30 m, as illustrated in Fig. 4d. It is evident that the topmost layer reveals a shear wave velocity estimate of 120 m/s. Towards deeper formations, the values of V_S increase up to 325 m/s. A similar trend in estimates of V_P values has also been observed. The V_P is found to be 300 m/s for the uppermost layer, having a thickness of 1 m.

9. LALCHAND BASTI

Figure 4e demonstrates the results of the observed SPAC curves. The uppermost layer which is of 3 m thickness shows a V_S value of 275 m/s,

whereas the estimate of V_P value for same layer is 500 m/s. The strata characterized by higher thickness yield the largest V_S value equal to 410 m/s. Similarly, the corresponding value of V_P is estimated to be 700 m/s. The shear wave velocity increases with depth along the profile. The corresponding dispersion curve for the fundamental mode of Rayleigh wave is provided in the same figure. The dispersion curve encompasses slowness estimates of 0.0026 to 0.0032 s/m.

Apart from the inversion of spatial autocorrelation ratios, we have extended our evaluation of shear wave velocity profiles through another robust technique.

10. INVERSION OF *H*/*V* ELLIPTICITY

The *H*/*V* ratio generally exhibits a peak that corresponds more or less to the fundamental frequency of the site ($f_0 = V_S/4h$; Bonnefoy-Claudet *et al.* 2004). Initially, the ratio is influenced by the S_H resonance in the superficial layers. If large contribution comes from Rayleigh surface waves, the theoretical ellipticity dictates the observed one as observed by Nogoshi and Igarashi (1970), Fäh *et al.* (2001, 2003), Scherbaum *et al.* (2003). Malischewsky and Scherbaum (2004) developed an analytical formulation for two-layer models. They plotted the differences of the peak frequency between the aforementioned surmises *versus* the magnitude of the velocity contrast. At intermediate and low contrasts, a drastic gap may exist between the two interpreta-tions. Additionally, the observed *H*/*V* peak better fits with the extremes of the *SH* transfer function, as inferred by Bonnefoy-Claudet *et al.* (2004). The usefulness of the *H*/*V* ratio method has been emphasized in several works. As pointed out by Nakamura (2008), this ratio is capable of yielding reliable estimates of the predominant frequency irrespective of the location of the site involving either ambient noise or earthquake motion as input. The *H*/*V* spectrum contains valuable information concerning the underlying structure, such as the relation between the V_S of the sediments and their thickness (Boore and Toksoz 1969, Scherbaum *et al.* 2003). On the other hand, the elliptiicty or S_H transfer function does not provide reliable information related to the site-specific amplification (Wathelet *et al.* 2005). The peak frequency is utilized to serve the objective of attaining the shear wave velocity structure. The V_P profile could be constrained to a good limit by exploiting the ellipticity amplitude.

11. INVERSION RESULTS FROM ELLIPTICITY OF *H*/*V* PEAK

Out of the five array sites, peak resonant frequency has been estimated through the horizontal to vertical ratio methodology only for three sites,

namely NEHU campus, Rylbang and Polo-ground. The resonant frequencies for these were previously estimated through single station method (Biswas and Baruah 2011) while for the remaining sites, we lacked resonant frequency estimates. The estimated peak resonant frequencies corresponding to these three sites are inverted in order to obtain the shear wave velocity model. The results for each array site are described below.

12. POLO-GROUND

When the H/V peak frequency that corresponds to this site is inverted, it produces a shear wave velocity profile characterized by increased values, as illustrated in Fig. 5a. The V_P and V_S values for the top layer, with a thickness of 1 m, are estimated to be 460 and 135 m/s, respectively. The next layer reveals a shear wave velocity of 210 m/s, corresponding to the V_P value of 515 m/s. The shear wave velocity to depth profile has been modeled up to the depth of 31 m for this site. The highest shear wave velocity has been found to be 375 m/s at the bottom stratum whose thickness is ~15 m. The dispersion curve resulting from the inversion shows an increase of slowness values with frequency. The slowness estimates range from 0.001 to 0.005 s/m.

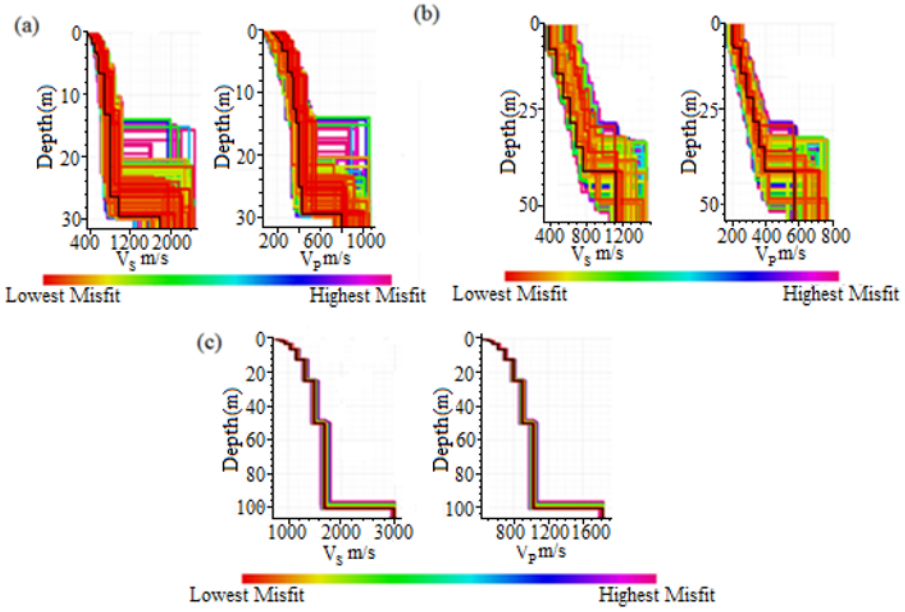

Fig. 5. Shear wave velocity profile estimated from H/V ellipticity: (a) Polo Ground, (b) Nehu, and (c) Rylbang.

13. NEHU

With the objective of attaining V_P and Vs profiles for NEHU, the corresponding peak frequency has been inverted. The obtained shear wave velocity model is displayed in Fig. 5b. The V_P and V_S values pertaining to the lowest misfit are considered. In this site, the shear wave velocity has been found to be 160 m/s for the top layer with a thickness of 8.5 m. Afterwards, a slow increase in the estimates of shear wave velocity pertaining to the site is observed. Similarly, the V_P values are also found to be very low for this site, having magnitude of 385 m/s for the surface layer.

14. RYLBANG

So far the H/V ratio estimates have been concerned; the fundamental frequency was observed to be at 7 Hz. The inversion results are demonstrated in Fig. 5c. The V_S shows a constant increase revealing a value of 525 m/s corresponding to the top layer, having a thickness of 4 m, whereas the bottom layer of thickness equal to 51 m is characterized by a value of 925 m/s. Concerning V_P, the top layer exhibits a value of 975 m/s, whereas the layer having higher thickness yields a value of 1560 m/s. Here, in accordance with the higher estimates of phase velocities, the curve provides small slowness values, starting from 0.0008 s/m.

All these observations suggest that the results from the inversion of peak resonant frequencies for these array sites are in a general agreement with the shear wave velocity profiles and the dispersion curves. The application of all procedures produces comparable results, irrespective of their variant inherent computation procedures.

15. CORRELATION WITH GEOPHYSICAL AND GEOTECHNICAL PARAMETERS

The estimated shear wave velocity models obtained through these different techniques are compatible. However, this estimation requires validation through correlation with available geophysical and geotechnical information. In this regard, such information like borehole, resistivity and gravity data is compared with the shear wave velocity models estimated for Shillong City.

Concerning geotechnical information, the report on the resistivity profile, available for the Raj-bhaban Area by the Central Ground Water Board (CGWB 2008), Shillong, indicates higher resistivity values at depths of 20-30 m (Fig. 6). The values obtained in these depths are observed to be in the range of 2650 to 6500 ohm-m, as indicated in the table of Fig. 6. These higher values of resistivity imply the existence of stiff soil strata overlain by basement rock (Lay and Wallace 2001), where the shear wave velocity increases with the compactness of the strata. In accordance with the obtained

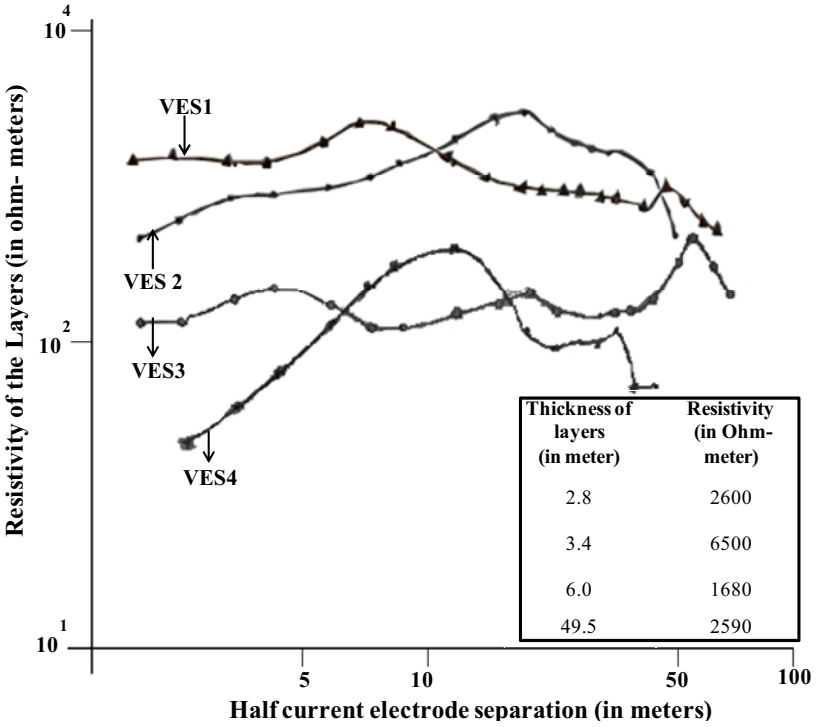

Fig. 6. Resistivity profile of the Rajbhaban Area (after Report by CGWB 2008). In the bottom right corner, the corresponding resistivity values are provided for this site. Resistivity is provided against each layer in ohm-meter units.

results, higher shear wave velocity values are obtained at Rylbang, which is in the vicinity of Rajbhaban Area.

Other geophysical investigations have also been carried out both in and around Shillong City. For example, geophysical investigations, including magmatic, resistivity, and gravity ones, were executed in an area covering 6 km^2 by the Geological Survey of India (GSI 1985, Dasgupta and Biswas 2000, Kalita 1998). Their study reveals a zone of low resistivity and moderate gravity anomaly of 0.3 mGal in the NEHU campus. It is attributed to the existence of a localized region of carbonaceous phylites up to depths of 102 to 139 m. This observation is found to be consistent with the derived shear wave velocity models in this work. According to their conjecture, this region extends up to 3.2 km in the Shillong area. This observation is consistent with the shear wave velocity models derived in this work. Generally, areas yielding low resistivity are considered as low velocity zones, *i.e.*, shear wave velocity decline because of lower porosity and lower density pertinent to

stratum. The V_S values estimated by the inversion of the SPAC, corresponding to the NEHU site, are observed to be relatively low, in the range of 150 to 300 m/s. However, towards the other side of the Shillong area, a study of GSI (1985) inferred the abundance of metabasic rocks such as quartzite and phyllites, which present higher resistivity values. In accordance with this observation, the derived model exhibits higher values of shear wave velocities in accordance with the results of geophysical investigation.

Additionally, the shear wave estimates computed through empirical relationship incorporating geotechnical parameters in the form of N values from Standard Penetration Test are found to be in good agreement with the estimates obtained through these inversion techniques (see Biswas *et al.* 2015). As an example, the Lalchand Basti site can be considered. As shown in Fig. 7, the empirically determined (Ohta and Goto 1978) shear wave velocity profile matches reasonably well the models obtained through the inversion. It is evident in this figure that V_S has been empirically estimated to be in the range of 250 to 475 m/s, while in the shear wave velocity models evaluated

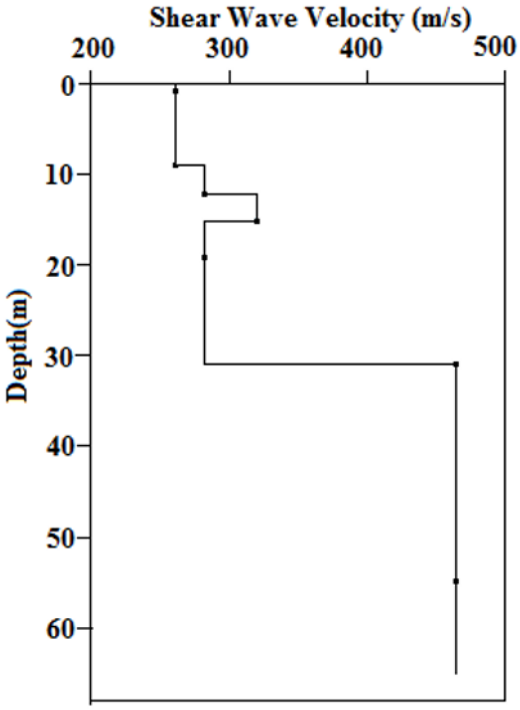

Fig. 7. Shear wave velocity profile for Lalchand Basti site estimated through empirical relationship. Depth is plotted along the vertical axis whereas the empirically computed shear wave velocities are provided along the horizontal axis.

through inversion a similar range of V_S values is obtained, *i.e.*, 245 to 435 m/s. Thus, the derived shear wave velocity models present good correlation with the geotechnical parameters.

Simultaneously, the geological map, as well as the available borehole information, is found to be in good agreement with the estimates of V_P and V_S profiles as obtained by the inversion in the other array sites, such as POLO-GROUND or ASSAM HOUSE.

16. DISCUSSIONS

In this study, we endeavor to assess the shallow shear wave velocity structure of Shillong City with simultaneous determination of subsurface V_P values, to a lesser extent, using ambient noise wavefield. Two different methodologies are adopted, namely the Spatial Autocorrelation Method and the H/V peak inversion where the phase velocity dispersion curves are inverted to estimate the desired profile. The inverted profiles (V_S and V_P values) are separately determined from the SPAC curves and frequency-wavenumber curves for the five sites. These velocity structures, computed using these methods, are compared for consistency with the velocity profile estimated from H/V peak frequency inversion. The estimated velocity profiles are then correlated with available geophysical information.

The computed SPAC estimates exhibit a varying pattern. In all the five sites, the average autocorrelation ratios are found to be in the range of ± 0.3. As per Okada (2006), three stations or more is the best array deployment towards estimating SPAC coefficients corresponding to fundamental mode. Here, we also constrain the estimates to the first minimum by adoption of four station strategy. The obtained results can be related to the discussion of errors in SPAC coefficient by Henstridge (1979) and Matsuoka *et al.* (1996). However, there is plausibility in augmenting more coherent arrivals for determining SPAC coefficients by adding more stations.

The SPAC ratios in two of the sites, Rylbang and Assam House, reveal high scatter. In a similar work by Asten *et al.* (2004), noticeable scatter in the SPAC curves was observed, which had been attributed to a lack of source azimuthal coverage. In these two sites, the observed high standard deviations could be correlated to shorter time windows which actually generates side-effects. Another plausible explanation of this observation may be related to the insufficient energy at low frequencies (Wathelet *et al.* 2005). However, relatively less scatter is observed in Lalchand Basti, Polo-ground, and Nehu. These sites are characterized by less transients in the evaluated frequency band arising from ambient noise.

Subsequent to the inversion of the autocorrelation curves and ellipticity curves computed through SPAC and H/V, respectively, the shear wave ve-

locity to depth profile has also been estimated at each of the array sites. Simultaneously, V_P profiles are also estimated to a reliable extent. While deriving the shear wave velocity models, it is emphasized that the incorporation of the lithological information greatly improves the results (Wathelet *et al.* 2005). Out of the five array sites, sufficient geotechnical information in the form of borehole data was available for three sites (Polo-ground, Nehu, and Lalchand Basti). Shear wave velocity models are derived for these three sites based on the available information. Because of the inadequacy of lithological information at the other two sites (Rylbang and Assam House), the shear wave velocity models are interpolated from the available lithological information pertaining to three sites. In these two sites, the estimate of the sediment thickness is not well constrained. Further, for these two sites the results have lower accuracy. Similar observation was also reported by Scherbaum *et al.* (2003).

The computation of the estimated models through SPAC and H/V technique are found to be quite similar for four sites, except Rylbang. Additionally, the inversion of ellipticity of H/V peak resonant frequencies at the sites POLO-GROUND, RYLBANG, and NEHU yields shear wave models which are quite consistent with the results obtained through inversion of SPAC. The observations found from H/V peak inversion are quite comparable with other studies such as Fäh *et al.* (2003) and Bonnefoy-Claudet *et al.* (2008). Concerning the shear wave models, the estimates of V_P and V_S values are found to be of higher magnitude compared to the inversion results from SPAC. As pointed out by Ohnberger *et al.* (2004b), this may be related to the bias in the estimate of H/V peak frequency, which is the prime input for the inversion process, caused by external perturbation, such as strong wind or rain at the time of ambient noise survey (Hartzell 1992, Milana *et al.* 1996). It should be mentioned that there was continuous rain and wind during the ambient noise survey at Rylbang station.

Bonnefoy-Claudet *et al.* (2006) pointed out that there is a good agreement between the H/V ratio peak frequency, the fundamental frequency and ellipticity peak frequency of the fundamental Rayleigh Mode. In this study, almost all the inverted models, derived from SPAC curves and ellipticity inversion of H/V peak frequencies, show estimates of V_P and V_S values which are found to increase with depth. Several researchers reported this trend of subsurface shear wave velocities (Wathelet *et al.* 2004, Scherbaum *et al.* 2003). As in the work of Tokimatsu *et al.* (1992) and Tokimatsu (1997), it was postulated that there existed a mixture of fundamental and higher-mode dispersion curves, which would result in overestimation or underestimation of phase velocity estimates in the dispersion data and could remain undetected by the analyst's quality control. Even though it cannot be completely ruled out that there may be an overestimation of shear wave velocities in the

proposed ambient vibration model as obtained in Rylbang, most likely due to bias in the estimation of sediment/bedrock interface depth.

The thickness variations underneath the arrays significantly perturb the dispersion curves, so that the laterally unvarying 1D assumption is too strong and affects the results (Cornou *et al*. 2003, Cho *et al.* 2004). Since the fundamental mode of Rayleigh wave is taken into account due to incorporation only of the vertical component in all the inversion process through these two different methodologies, it is possible that higher modes of surface waves can be present in ambient vibrations, as observed by Tokimatsu (1997) and Zywicki (1999). On the other hand, some small contribution of higher modes at higher frequencies may occur, as indicated by Asten *et al.* (2004). Therefore, the derived shear wave velocity models and V_P values are constrained using only the vertical component for the five array sites. However, it can be stated with emphasis that the shear wave velocity models derived for each respective sites by these two techniques are in conformity.

In addition to the derivation of shear wave velocity models through these techniques, the obtained models are correlated with the available geotechnical and geophysical information. As for the NEHU site, the inverted model is in general agreement with resistivity values, as in the case of the Rylbang site. Apart from this, the shear wave velocity profiles empirically determined

Table 6

Comparison of shear wave velocities from different literature sources

Reference	Site geology	Computed velocity profiles V_S	In this study
Claprood and Asten 2010	Quarternary and Tertiary sediments	400-500 m/s within 0-50 m	Average 250-650 m/s up to 50 m depth
Chávez-Garcia *et al*. 2006	Sediments with clayey soil	530 m/s at 35 m; 700 m/s at 78 m	
Garcia-Jerez *et al*. 2007	Similar	250-750 m/s up to 200 m depth	
Roberts and Asten 2008	Quaternary sediments	200-500 m/s	
Rayhani *et al.* 2008	Same	100-600 m/s up to 35 m depth	
Louie 2001	Quaternary sediments	200-600 m/s	
Asten 2006	Sediments	300-800 m/s up to 280 m depth	

by us, following Ohta and Goto (1978), tally with the computed models. Another validation of the shear wave velocity estimates comes from the comparison of similar work by different researchers, as illustrated in Table 6. In Table 6, the estimates of shear wave velocities computed by them are listed. While presenting their results, it is kept in mind that the shear wave velocity estimates must correspond to the same lithology, irrespective of the geographic location of the sites. All these studies yield values which are found to be in good agreement with the computed shear wave velocities for the study area. Apart from this, it is observed that all SPAC curves yield SPAC ratios that exhibit a decaying pattern when approaching the higher frequency band. Several researchers, *e.g.*, Wathelet *et al.* (2004), Bard (2004), Bettig *et al.* (2001), and Raptakis and Makra (2010), have reported such observations. However, the stratification observed in the velocity profiles estimated by three techniques matches quite well the stratification of the sites Pologround, Rylbang, and Nehu, as observed in the lithology (as, for example, Table 7 highlighting NEHU).

Table 7a

Estimates of parameters for each layer as per spatial autocorrelation technique for array site NEHU

Layer	Thickness [m]	V_P [m/s]	V_S [m/s]
1	8.5	390	120
2	7	485	130
3	9	525	155
4	8	555	170
5	8	595	185
6	8	685	210

Table 7b

Interpretation of each layer as per ellipticity inversion of H/V peak for array site NEHU

Layer	Thickness [m]	V_P [m/s]	V_S [m/s]
1	8.5	400	110
2	7	480	120
3	9	525	145
4	8	585	168
5	8	645	195
6	8	695	215

Although we did implement these two techniques, which are based upon different working principles, still, each of them is endowed with its merits and demerits. For example, SPAC procedure is basically suitable for spatial and time coherent signals. It can reliably infer one dimensional velocity estimates with a moderate impedance contrast. On the other hand, H/V method is found to suitably yield dispersion curves for sites which are characterized by a sharp contrast. Since our study area is characterized by sharp to moderate contrast, varying from site to site, we have been encouraged to adopt the joint inversion of dispersion curves yielded by both these methods to attain converging results.

17. CONCLUSION

In this work, we analyze ambient vibrations recorded by three component arrays located in Shillong City. Our aim is to exploit the wave field characteristics of the ambient vibrations and thereby obtain the inverted shear wave velocity models. Two processing methods have been adopted to retrieve the dispersion characteristics from the recorded ambient vibrations. In all cases, the vertical components of the ambient vibrations were processed to obtain the V_S profile. The combined application of two techniques allowed us to attain a suitable shear wave velocity model compatible to the study region (Shillong City). The investigation carried out in this work has shown that it is possible to derive a velocity model of *S*-wave velocity structure for the study area by means of low cost measurements of ambient noise. Our results are consistent with other available data. The computed V_S values up to a depth of 30 m are found to be ~ 375 m/s, in most of the sites. This low value implies prevalence of a low velocity zone at some pocket areas, as supported by evidence of site-geology and geotechnical information. Moreover, in a recent publication (Biswas *et al.* 2015), we have established prevalence of low velocity zones from empirical estimation of observed H/V resonance frequencies. Thus, the smaller V_S estimates, as found in this study, eventually complements those as reported in Biswas *et al.* (2015).

More input from seismic reflection and refraction studies would enhance the reliability of the results. Despite the lack of *a priori* information of V_P and V_S values at two of the sites, we could retrieve the velocity to depth profiles.

The results provide fair insight towards understanding the subsurface and seismic hazard of the region. A further extension to a 2D and 3D model of the *S*-wave velocity profile obtained in this study would allow for improved knowledge of the interior of the depth profiles, which would be the focus of future research.

References

Aki, K. (1957), Space and time spectra of stationary waves with special reference to micro tremors, *Bull. Earth. Res. Inst. Univ. Tokyo* **35**, 415-456 (in Japanese).

Asten, M.W., T. Dhu, and N. Lam (2004), Optimized array design for microtremor array studies applied to site classification; comparison of results with SCPT logs. **In:** *Proc. 13th World Conf. on Earthquake Engineering, Vancouver, Canada*, Paper No. 2903.

Asten, M.W. (2006), On bias and noise in passive seismic data from finite circular array data processed using SPAC methods, *Geophysics* **71**, 6, V153-V162.

Bard, P.Y. (2004), The SESAME project: an overview and main results. **In:** *13th World Conf. on Earthquake Engineering, August 2004, Vancouver, Canada*, paper No. 2207.

Bettig, B., P.Y. Bard, F. Scherbaum, J. Riepl, F. Cotton, C. Cornou, and D. Hatzfeld (2001), Analysis of dense array noise measurements using the modified spatial auto-correlation method (SPAC): Application to the Grenoble area, *Boll. Geofis. Teor. Appl.* **42**, 3-4, 281-304.

Biswas, R., and S. Baruah (2011), Site response estimation by Nakamura method: Shillong City, Northeast India, *Mem. Geophys. Soc. India* **77**, 173-183.

Biswas, R., S. Baruah, and D.K. Bora (2013), Influence of attenuation and site on microearthquakes' spectra in Shillong region of Northeast India: A case study, *Acta Geophys*. **61**, 4, 886-904, DOI: 10.2478/s11600-013-0129-x.

Biswas, R., S. Baruah, and D.K. Bora (2015), Mapping sediment thickness in Shillong City of northeast India, through empirical relationship, *J. Earthq.* **2015**, 572619, DOI: 10.1155/2015/572619.

Bonnefoy-Claudet, S., C. Cornou, J. Kristek, M. Ohrnberger, M. Wathelet, P.-Y. Bard, P. Moczo, D. Fah, and F. Cotton (2004), Simulation of seismic ambient noise: I. Results of H/V and array techniques on canonical models. **In:** *Proc. 13th World Conf. on Earthquake Engineering.*

Bonnefoy-Claudet, S., F. Cotton, and P.Y. Bard (2006), The nature of the seismic noise wave field and its implication for site effects studies, a literature review, *Earth Sci. Rev*. **79**, 205-227.

Bonnefoy-Claudet, S., F. Leyton, S. Baize, C. Berge-Thierry, L.F. Bonilla, and J. Campos (2008), Potentiality of microtremor to evaluate site effects at shallow depths in the deep basin of Santiago de Chile. **In:** *Proc. 14th World Conf. on Earthquake Engineering, 12-17 October 2008, Beijing, China.*

Boore, D.M., and M.W. Asten (2008), Comparisons of shear-wave slowness in the Santa Clara Valley, California, using blind interpretations of data from invasive and noninvasive methods, *Bull. Seismol. Soc. Am.* **98**, 4, 1983-2003, DOI: 10.1785/0120070277.

Boore, D.M., and M.N. Toksoz (1969), Rayleigh wave particle motion and crustal structure, *Bull. Seismol. Soc. Am.* **59**, 1, 331-346.

Borcherdt, R.D. (1970), Effects of local geology on ground motion near San Francisco Bay, *Bull. Seismol. Soc. Am.* **60**, 1, 29-61.

Bozdag, E., and A.H. Kocaoglu (2005), Estimation of site amplification from shear wave velocity profiles in Yesilyurt and Avcilar, Istanbul by frequency-wavenumber analysis of microtremors, *J. Seismol.* **9**, 1, 87-98, DOI: 10.1007/s10950-005-5271-8.

Campbell, K.W. (1976), A note on the distribution of earthquake damage in Long Beach, 1933, *Bull. Seismol. Soc. Am.* **66**, 3, 1001-1006.

CGWB (2008), Geophysical profiling of Greater Shillong Area, Central Ground Water Board, Shillong (unpublished report).

Chattopadhaya, N., and S. Hashimi (1984), The Sung valley alkaline ultramaffic carbonatite complex, East Khasi Hills district, Meghalaya, *Rec. Geo. Surv. In.* **113**, 4, 24-33.

Chávez-García, F.J., M. Rodríguez, and W.R. Stephenson (2006), Subsoil structure using SPAC measurements along a line, *Bull. Seismol. Soc. Am.* **96**, 2, 729-736, DOI: 10.1785/0120050141.

Cho, I., T. Tada, and Y. Shinozaki (2004), Suggestion and theoretical evaluations on the performance of a new method to extract phase velocities of Rayleigh waves from microtremor seismograms obtained with a circular array. **In:** *13th World Conference on Earthquake Engineering*, Paper No. 647.

Claprood, M., and M.W. Asten (2007a), Use of SPAC, HVSR and strong motion analysis for site hazard study over the Tamar Valley in Launceston, Tasmania. **In:** *Earthquake Engineering in Australia Conference*.

Claprood, M., and M.W. Asten (2007b), Combined use of SPAC, FK and HVSR microtremor survey methods for site hazard study over the Tamar Valley in Launceston, Tasmania. **In:** *ASEG 19th Geophysical Conference and Exhibition, Perth, Australia*, Extended abstracts.

Claprood, M., and M.W. Asten (2010), Statistical validity control on SPAC microtremor observations recorded with a restricted number of sensors, *Bull. Seismol. Soc. Am.* **100**, 2, 776−791, DOI: 10.1785/0120090133.

Cornou, C., P.-Y. Bard, and M. Dietrich (2003), Contribution of dense array analysis to the identification and quantification of basin-edge-induced waves. Part I: Methodology, *Bull. Seismol. Soc. Am.* **93**, 6, 2604-2623, DOI: 10.1785/0120020139.

Dasgupta, A., and A. Biswas (2000), *Geology of Assam*, Geological Society of India, Bangalore.

Di Giulio, G., C. Cornou, M. Ohrnberger, M. Wathelet, and A. Rovelli (2006), Deriving wavefield characteristics and shear velocity profiles from two dimensional small aperture arrays analysis of ambient vibrations in a small size alluvial basin, Colfiorito, Italy, *Bull. Seismol. Soc. Am.* **96**, 5, 1915-1933, DOI: 10.1785/0120060119.

Fäh, D., F. Kind, and D. Giardini (2001), A theoretical investigation of average H/V ratios, *Geophys. J. Int.* **145**, 2, 535-549.

Fäh, D., F. Kind, and D. Giardini (2003), Inversion of local S-wave velocity structures from average H/V ratios, and their use for the estimation of site effects, *J. Seismol.* **7**, 4, 449-467, DOI: 10.1023/B:JOSE.0000005712.86058.42.

Garcia-Jerez, A., M. Navarro, F.J. Alcala, F. Luzon, J.A. Perez Ruiz, T. Enomoto, F. Vidal, and E. Ocana (2007), Shallow velocity structure using joint inversion of array and h/v Spectral ratio of ambient noise, The case of Mula Town (SE of Spain), *Soil Dyn. Earthq. Eng*. **27**, 907-919.

GSI (1985), Geology mapping in greater Shillong area, Meghalaya, Memoir Geolog. Surv. India.

Hartzell, S.H. (1992), Site response estimation from earthquake data, *Bull. Seismol. Soc. Am.* **82**, 6, 2308-2327.

Hartzell, S.H., P. Liu, and C. Mendoza (1996), The 1994 Northridge, California earthquake: Investigation of rupture velocity, rise time, and high-frequency radiation, *J. Geophys. Res.* **101**, B9, 20091-20108, DOI: 10.1029/96JB01883.

Henstridge, D.J. (1979), A signal processing method for circular arrays, *Geophysics* **44**, 2, 179-184, DOI: 10.1190/1.1440959.

Herak, M. (2008), ModelHVSR: a Matlab_ tool to model horizontal-to-vertical spectral ratio of ambient noise, *Comput. Geosci.* **34**, 11, 1514-1526, DOI: 10.1016/j.cageo.2007.07.009.

Kalita, B.C. (1998), Ground water prospects of Shillong Urban Aglomerate, Central Ground Water Board, Meghalaya (unpublished report).

Kassaras, I., D. Kalantoni, Ch. Benetatos, G. Kaviris, K. Michalaki, N. Sakellariou, and K. Makropoulos (2015), Seismic damage scenarios in Lefkas old town (W. Greece), *Bull. Earthq. Eng.* **13**, 12, 3669-3711, DOI: 10.1007/s10518-015-9789-z.

Kayal, J.R. (2008). *Microearthquake Seismology and Seismotectonics of South Asia*. Springer, Dordrecht.

Kayal, J.R., S.S. Arefiev, S. Baruah, D. Hazarika, N. Gogoi, A. Kumar, S.N. Chowdhury, and S. Kalita (2006), Shillong Plateau Earthquakes in northeast India region: Complex tectonic model, *Curr. Sci.* **91**, 1, 109-114.

Köhler, A., M. Ohrnberger, F. Scherbaum, M. Wathelet, and C. Cornou (2007), Assessing the reliability of the modified three-component spatial autocorrelation technique, *Geophys. J. Int.* **168**, 2, 779-796, DOI: 10.1111/j.1365-246X.2006.03253.x.

Kuo, C.H., D.S. Cheng, H.H. Hsieh, T.M. Chang, H.J. Chiang, C.M. Lin, and K.L. Wen (2009), Comparison of three different methods in investigating shallow shear-wave velocity structures in Ilan, Taiwan, *Soil Dyn. Earthq. Eng.* **29**, 1, 133-143.

Lay, T., and T.C. Wallace (2001), *Modern Global Seismology*, Academic Press.

Louie, L.N. (2001), Faster, better: Shear wave velocity to 100 meters depth from refraction microtremor arrays, *Bull. Seismol. Soc. Am*. **91**, 347-364.

Malischewsky, P.G., and F. Scherbaum (2004), Love's formula and H/V-ratio (ellipticity) of Rayleigh waves, *Wave Motion* **40**, 1, 57-67, DOI: 10.1016/j.wavemoti.2003.12.015.

Matsuoka, T., N. Umezawa, and H. Makishima (1996), Experimental studies on the applicability of the spatial autocorrelation method for estimation of geological structures using microtremors, *Butsuri Tansa* **49**, 26-41.

Milana, G., S. Barba, D.E. Pezzo, and E. Zambonelli (1996), Site response from ambient noise measurements: new perspectives from an array study in Central Italy, *Bull. Seismol. Soc. Am.* **86**, 2, 320-328.

Mitra, S., and C. Mitra (2001), Tectonic setting of the precambrians of the northeastern India, Meghalaya Plateau, and age of Shillong group of rocks, *Geol. Surv. India Spec. Publ.* **64**, 653-658.

Nakamura, Y. (2008), On the H/V Spectrum. **In:** *14th World Conf. on Earthquake Engineering.*

Nogoshi, M., and T. Igarashi (1970), On the propagation characteristics of microtremors, *J. Seismol. Soc. Jap.* **23**, 264-280.

Ohnberger, M., E. Schissele, C. Cornou, M. Wathelet, A. Savvaidis, F. Scherbaum, D. Jongmans, and F. Kind (2004a), Microtremor array measurements for site effect investigations: comparison of analysis methods for field data crosschecked by simulated wavefields. **In:** *13th World Conf. on Earthquake Engineering, 1-6 August 2004, Vancouver, Canada*, Paper No. 0940.

Ohnberger, M., F. Scherbaum, F. Krüger, R. Pelzing, and Sh.-K. Reamer (2004b), How good are shear wave velocity models obtained from inversion of ambient vibrations in the Lower Rhine Embayment (NW-Germany), *Boll. Geof. Teor. Appl.* **45**, 3, 215-232.

Ohta, Y., and N. Goto (1978), Empirical shear wave velocity equations in terms of soil characteristics soil indexes, *Earthq. Eng. Struct. Dyn.* **6**, 167-187.

Okada, H. (2006), Theory of efficient array observations of microtremors with special reference to the SPAC method, *Explor. Geophys.* **37**, 1, 73-84, DOI: 10.1071/EG06073.

Papadopoulou-Vrynioti, K., G. Bathrellos, H. Skilodimou, G. Kaviris, and K. Makropoulos (2013), Karst collapse susceptibility mapping considering peak ground acceleration in a rapidly growing urban area, *Eng. Geol.* **158**, 77-88, DOI: 10.1016/j.enggeo.2013.02.009.

Pavlou, K., G. Kaviris, K. Chousianitis, G. Drakatos, V. Kouskouna, and K. Makropoulos (2013), Seismic hazard assessment in Polyphyto Dam area (NW Greece) and its relation with the "unexpected" earthquake of 13 May 1995 (Ms = 6.5, NW Greece), *Nat. Hazards Earth Syst. Sci.* **13**, 141-149, DOI: 10.5194/nhess-13-141-2013.

Picozzi, M., S. Parolai, and D. Albarello (2005), Statistical analysis of noise horizontal-to-vertical spectral ratios (HVSR), *Bull. Seismol. Soc. Am*. **95**, 5, 1779-1786, DOI: 10.1785/0120040152.

Rao, J.M., and G.V.S.P. Rao (2008), Geology, geochemistry and palaeomagnetic study of cretaceous mafic dykes of Shillong Plateau and their evolutionary history. **In:** R.K. Srivastava, Ch. Sivaji, and N.V. Chalapathi Rao (eds.), *Indian Dykes: Geochemistry, Geophysics and Geomorphology*, Narosa Publishing House, 589-607.

Raptakis, D., and K. Makra (2010), Shear wave velocity structure in western Thessaloniki (Greece) using mainly alternative SPAC method, *Soil Dyn. Earthq. Eng*. **30**, 4, 202-214, DOI: 10.1016/j.soildyn.2009.10.006.

Rayhani, M.H.T., M.H. El Naggar, and S.H. Tabatabi (2008), Nonlinear analysis of local site effects on seismic ground response in the Bam earthquake, *Geotech. Geolog. Eng.* **21**, 1, 91-100.

Roberts, J., and M.W. Asten (2008), A study of near source effects in array-based (SPAC) microtremor surveys, *Geophys. J. Int*. **174**, 1, 159-177, DOI: 10.1111/j.1365-246X.2008.03729.x.

Sambridge, M. (1999a), Geophysical inversion with a neighborhood algorithm. I. Searching a parameter space, *Geophys. J. Int.* **138**, 2, 479-494, DOI: 10.1046/j.1365-246X.1999.00876.x.

Sambridge, M. (1999b), Geophysical inversion with a neighborhood algorithm. II. Appraising the ensemble, *Geophys. J. Int.* **138**, 3, 727-746, DOI: 10.1046/j.1365-246x.1999.00900.x.

Sar, S.N. (1973), An interim report on ground water exploration in the Greater Shillong area, Khasi Hills District, Meghalaya, Memo report, Central Ground Water Board.

Scherbaum, F., K.G. Hinzen, and M. Ohrnberger (2003), Determination of shallow shear wave velocity profiles in the Cologne, Germany area using ambient vibrations, *Geophys. J. Int.* **152**, 3, 597-612, DOI: 10.1046/j.1365-246X.2003.01856.x.

Seligson, C.D. (1970), Comments on high-resolution frequency wavenumber spectrum analysis, *Proc. IEEE* **58**, 6, 947-949, DOI: 10.1109/PROC.1970.7825.

Srinivasan, P., S. Sen, and P.C. Bandopadhaya (1996), Study of variation of Paleocene-Eocene sediments in the shield areas of Shillong Plateau, *Rec. Geol. Surv. India* **129**, 77-78.

Tokimatsu, K. (1997), Geotechnical site characterization using surface waves. **In:** *Proc. 1st Int. Conf. on Earthquake Geotechnical Engineering*, Vol. 3, 1333-1368.

Tokimatsu, K., K. Shinzawa, and S. Kuwayama (1992), Use of short-period micro tremors for V_s profiling, *J. Geotech. Eng*. **118**, 10, 1554-1558, DOI: 10.1061/(ASCE)0733-9410(1992)118:10(1544).

Wathelet, M., D. Jongmans, and M.Ohrnberger (2004), Surface-wave inversion using a direct search algorithm and its application to ambient vibration measurements, *Near Surf. Geophys.* **2**, 4, 211-221, DOI: 10.3997/1873-0604.2004018.

Wathelet, M., D. Jongmans, and M. Ohrnberger (2005), Direct inversion of spatial autocorrelation curves with the neighborhood algorithm, *Bull. Seismol. Soc. Am*. **95**, 5, 1787-1800, DOI: 10.1785/0120040220.

Williams, R.A., W.J. Stephenson, and J.K. Odum (2003), Comparison of P- and S-wave velocity profiles obtained from surface seismic refraction/reflection and downhole data, *Tectonophysics* **368**, 1-4, 71-88, DOI: 10.1016/S0040-1951(03)00151-3.

Woods, J.W., and P.L. Lintz (1973), Plane waves at small arrays, *Geophysics* **38**, 6, 1023-1041, DOI: 10.1190/1.1440393.

Yamanaka, H., M. Dravinski, and H. Kagami (1993), Continuous measurements of microtremors on sediments and basement in Los Angeles, California, *Bull. Seismol. Soc. Am.* **83**, 5, 1595-1609.

Yamanaka, H., M. Takemura, H. Ishida, and M. Niwa (1994), Characteristics of long-period microtremors and their applicability in exploration of deep sedimentary layers, *Bull. Seismol. Soc. Am.* **84**, 6, 1831-1841.

Yamanaka, H., K. Irikura, K. Kudo, H. Okada, and T. Sasatani (1998), Geophysical explorations of sedimentary structures and their characterization. **In:** *Proc. 2nd Int. Symp. on the Effects of Surface Geology on Seismic Motion* **1**, 15-33.

Zywicki, D.J. (1999), Advanced signal processing methods applied to engineering analysis of seismic surface waves, Ph.D. Thesis, Georgia Institute of Technology, Atlanta, USA.

Received 28 April 2015
Received in revised form 3 February 2016
Accepted 8 February 2016